sciendo

CIVIL AND ENVIRONMENTAL ENGINEERING REPORTS

E-ISSN 2450-8594

CEER 2022; 32 (3): 0166-0181
DOI: 10.2478/ceer-2022-0034
Original Research Article

EVALUATION OF BEHAVIOR OF HYBRID BEAM COMBINING STEEL INVERTED T-SECTION AND RC FLANGE

Hacene BADACHE[1], Samy MEZHOUD[1]*, Abdul Qader MELHEM [2]
[1]Laboratoire Matériaux et Durabilité des Constructions (LMDC), Department of Civil Engineering, University of Mentouri Brothers Constantine 1, Constantine, Algeria
[2]Dept. of Civil Engineering Faculty of civil engineering, University of Aleppo, Syria

A b s t r a c t

This paper deals with flexural investigation of a type of steel-concrete composite beam structure able to provide an adequate bond between steel and concrete elements through the application of a simple steel reinforcement shear connector design, steel reinforcing bars bent into L-shapes. The cross sections involve inverted steel T-beam being embedded within reinforced concrete (RC) flange of the slab. The paper concentrates on elastic and elastic-plastic behaviour of steel inverted T-beam entrenched within a reinforced concrete flange at the top. In addition, shear connection was investigated in detail. Finally, some suggested designing equations and curves simulating the elastic, elastoplastic and full plastic experimental moments were developed. The plastic theoretical study results coincides with the experimental behaviour of the developed model.

Keywords: composite, steel-concrete, inverted T-beam, L-shaped connectors, elastic, plastic

* Corresponding author: University of Mentouri Brothers Constantine 1, Department of Spatial Planning, University of Mentouri Brothers Constantine 1, Constantine, Algeria, e-mail: mezhoud.sami@umc.edu.dz, Tél:+213 553 481 132

1. INTRODUCTION

Composite steel-concrete beams are typical structural elements present in both floor and bridge systems [1-6], and they're assessed using well-established methods and regulated by several code design around the world like *AISC* code [17] or Eurocode 4 [18].

The most conventional composite beam involves of a W-shape steel beam made composite with a concrete slab through headed shear studs. Under load, the headed studs transfer horizontal shear forces between the steel and concrete, causing the two parts to behave as if they were one composite member. The majority of studies has been done up to this point [7-13, 15] concerned with composite construction done on a concrete slab over top flange of steel beam. The mechanical shear connectors on top flange may be considered to be either flexible or rigid in ordinary composite construction industries. In the case of solution without headed studs, Remennikov and Roche [14] suggested that the L-shaped shear connectors were observed to deform in a similar way to that for the flexible headed stud shear connectors.

The flexible shear connectors are able to yield and undergo plastic deformation when resisting shear forces, making them more ductile than rigid connectors. On the other hand, the use of steel reinforcing bars as shear connectors is intended to provide a more worthwhile shear connection design than the commonly used headed studs [16].

As steel reinforcing bars are such a commonly utilized construction material, there is no need for the purchase of specially manufactured headed studs. In addition, as menthionned by Eurocode 4, these reinforcing bars should be in accordance with BS EN 10080 [18, 19]. Accordingly, steel reinforcing bars bent into L-shapes may be integrated into the design, spaced at a specific distance center to center in an alternately arrangement.

In this context, this paper deals with flexural investigation of a type of steel-concrete composite beam structure able to provide an adequate bond between steel and concrete elements through the application of a simple steel reinforcement shear connector design, steel reinforcing bars bent into L-shapes.

2. COMPOSITE SECTION PROPERTIES

2.1. Inverted T-steel section properties

A 150UB18.0 standard I- beam section was chosen to be cut along the web at the top root radius. Properties of this inverted T-steel beam are summarized in Fig.1. It is important to mention that when values are calculated neglecting roots there are a resulting difference in crosssectional area about 2% in comparison to precise value.

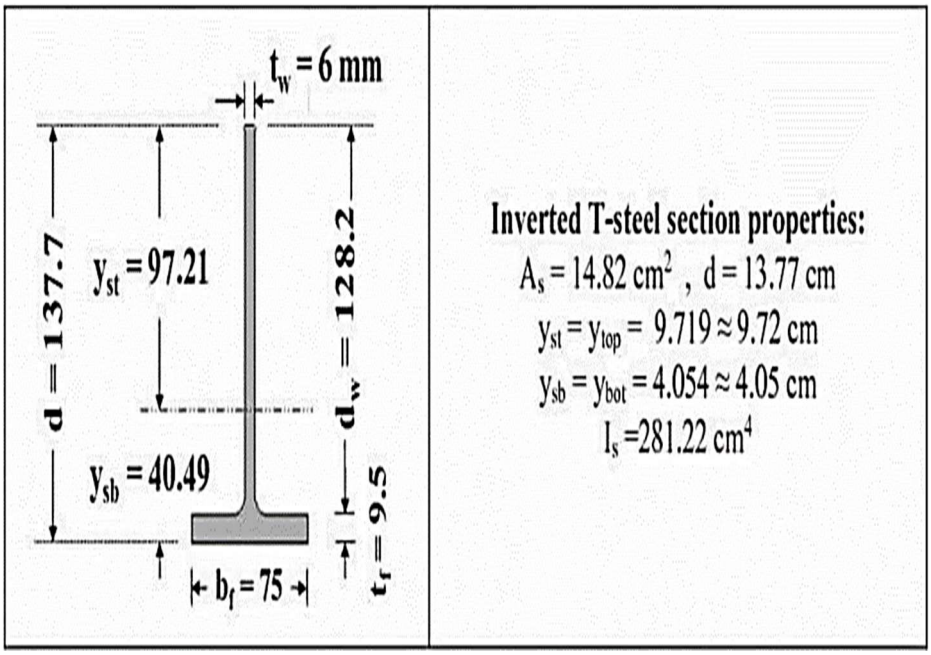

Fig. 1. Properties of inverted *T*-steel beam

2.2. Elastic analysis

The elastic properties of the composite section (T-section and RC flange) of Fig. 2 are calculated by the following equations:

The Modulus ratio:

$$n = E_s/E_c = 200000/[4729.77\sqrt{f_c'}] \geq 6 \quad (2.1)$$

For: $y = y_{top} \leq t_c$

$$y = y_{top} = 0.5\,\{-\frac{2n}{b_e}A_s + [(\frac{2n}{b_e}A_s)^2 + 4\frac{2n}{b_e}A_s(y_{st} + d')]^{1/2}\} \quad (2.2)$$

$$I_{tr} = \frac{b_e}{n}\frac{y^3}{3} + I_s + A_s[y_{st} + d' - y]^2 \quad (2.3)$$

For: $y = y_{lop} > t_c$

$$y = y_{top} = \frac{0.5b_e t_c^2 + nA_s[y_{st} + d']}{b_e t_c + nA_s} \quad (2.4)$$

$$I_{tr} = \frac{b_e}{n}\frac{t_c^3}{12} + \frac{b_e}{n}t_c[y - 0.5t_c]^2 + I_s + A_s[y_{st} + d' - y] \quad (2.5)$$

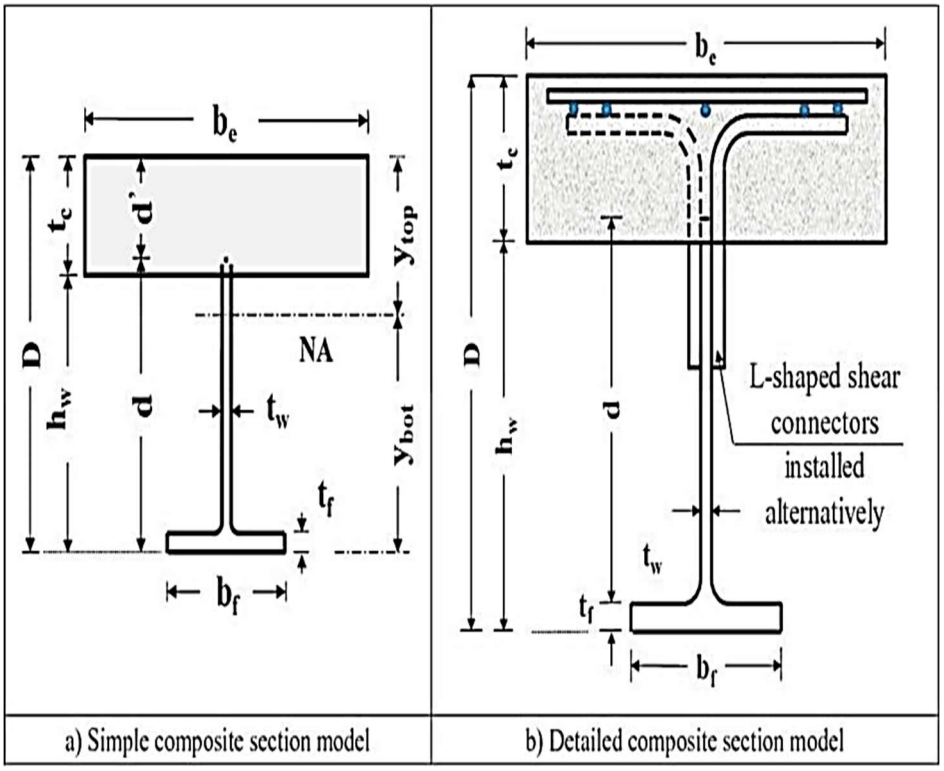

Fig. 2. Composite section model

The Resisting moment is the lesser value of (2.6) and (2.7):

$$\sigma_c' = \frac{My_{top}}{I_{tr}}\frac{1}{n}, M_c = \frac{0.45\ f_c' I_{tr} n}{y_{top}} \quad (2.6)$$

$$\sigma_s = \frac{My_{bot}}{I_{tr}}, M_s = \frac{0.66F_y I_{tr}}{y_{bot}} \quad (2.7)$$

Where:

- f_c' is the compressive strength of concrete,
- F_y is the yield strength of steel beam.

2.3. Elastic −Plastic analysis

If $y_{top} < y_{ba}$, in *Fig*. 3, the bottom tension fiber of steel section yields first. The bending moment and curvature angle are:

$$M_y = \frac{F_y\, I_{tr}}{v_{bot}} \text{ and } \phi_y = \tan^{-1}\left(\frac{\varepsilon_y}{y_{top}}\right) \tag{2.8}$$

If $y_{\text{top}} > y_{ba}$, the top compression fibre of concrete yields first. The bending moment and curvature angle are:

$$M_y = \frac{0.85\, f'_c\, I_{tr}\, n}{y_{top}} \text{ and } \phi_y = \tan^{-1}\left(\frac{\varepsilon'_c}{y_{top}}\right) \tag{2.9}$$

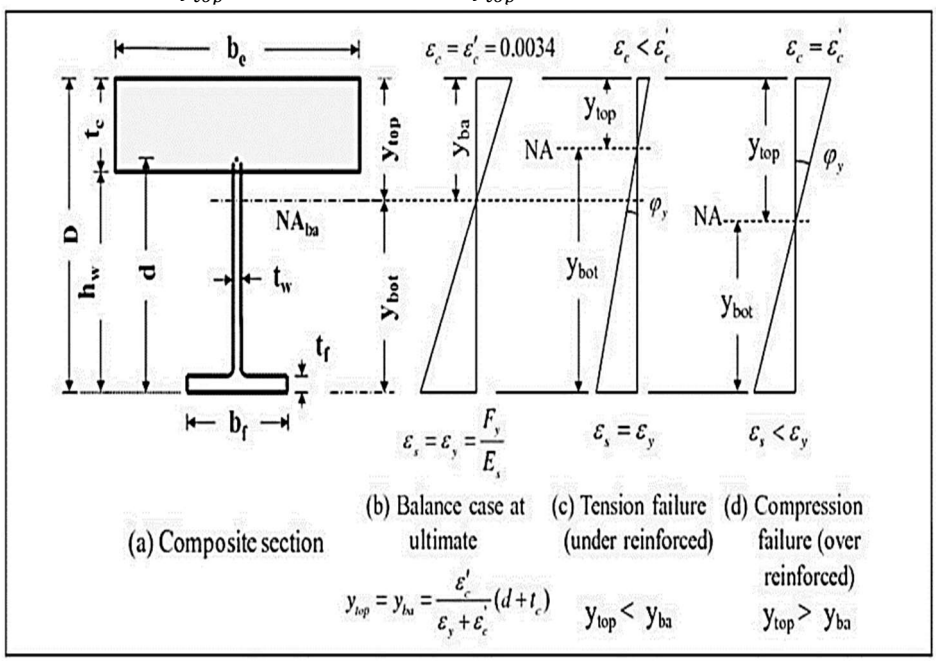

Fig. 3**.** Structural cases of the composite model

2.4. Shear connector analysis

For the following Fig.4, the shear connectors analysis may be outlined by *AISC-2010* [17] by these equations:

$$V_h = 0.85 f'_c b_e t_c \text{ or } V_h = A_S F_y \text{ (the smaller value)} \tag{2.10}$$

Number of shear connectors between support and mid-span (zero moment and adjacent maximum bending moment) is:

$$N_{stud} = V_h/[0.85q_{ult}] \tag{2.11}$$

Where: q_{ult} is ultimate shear strength of shear connector.

$$q_{ult} = 0.5\ A_{st}\sqrt{f_c' E_c} = 0.40\ d^2{}_{st}\sqrt{f_c' E_c} \tag{2.12}$$

d_{st} is shear connector diameter

E_c is modulus of elasticity of concrete.

The spacing of shear connectors along the beam is:

$$s = \frac{q_{stud}}{V_i Q/I_{tr}} n_{row} \leq S_{max} \tag{2.13}$$

n_{row} is number of L-shaped connector rows installed in a staggered prearrangement.

Q is static moment of slab about neutral axis.

$$Q = (b_e f n)k[y\iota_Q p - 0.5 l_c] \tag{2.14}$$

V_i is shear force at section i

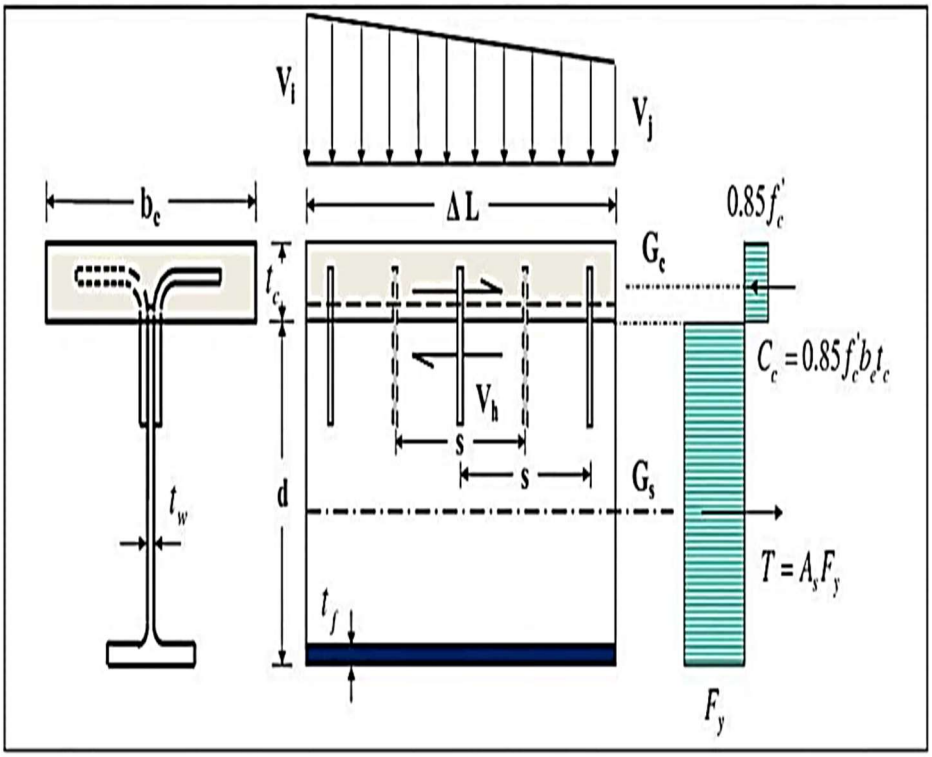

Fig. 4**.** Shear connector analysis showing L-shaped shear connector spacing

2.5. Plastic analysis

There are three cases in plastic analysis as shown in *Fig*. *5*, *6 and 7*.

Case 1:

PNA is within slab in *Fig*. *5*, where: $a \leq d'$

$$a = \frac{A_s F_y}{0.85 f_c' b_e}, \mathrm{M}_p = A_s \, \mathrm{F}_y \, [D - y_{sb} - \frac{1}{1.7} \frac{A_s}{b_e} \frac{F_y}{f_c'}] \tag{2.15}$$

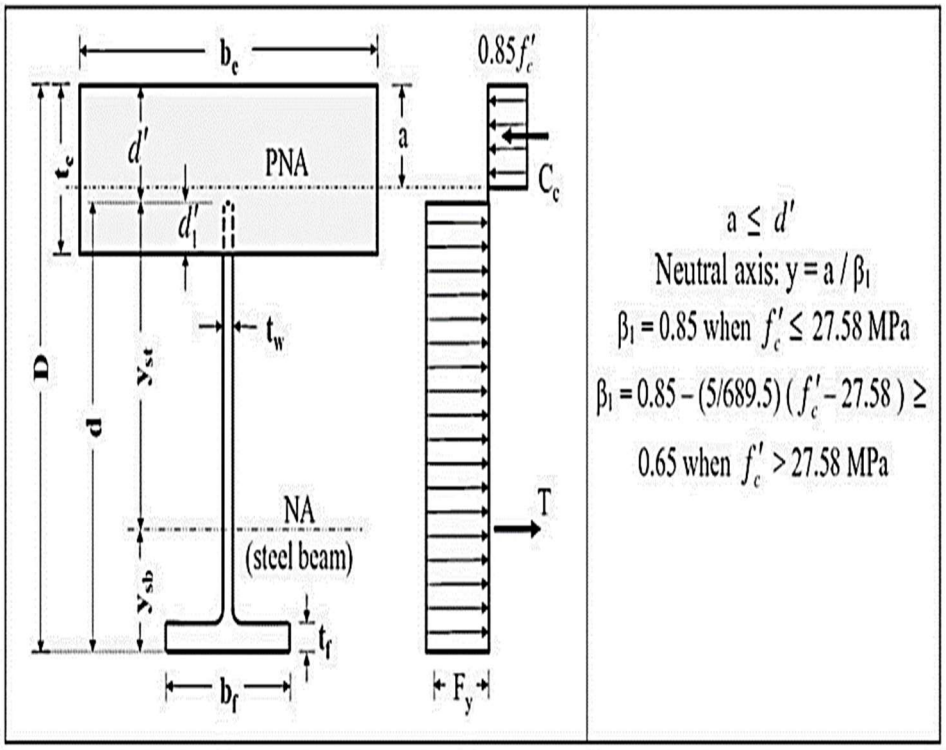

Fig. 5. Plastic neutral axis (PNA) is in the concrete flange, where: $a \leq d'$

It is important to mention that in this formula the value of 1.7 in denominator occur according to AISC practice. According to the Eurocode 4, aforementioned denominator would be 2.0.

Case 2:

PNA is in the web within slab in *Fig. 6*, where: $d' < a \leq t_c$

$$a = \frac{[t_w(d_w+2d')+A_f]F_y-0.85f'_c d' t_w}{0.85f'_c(b_e-t_w)+2t_w F_y} \tag{2.16}$$

$$y_{sb} = \frac{A_f[0.5t_f]+[d_w-(a-d')]t_w[t_f+0.5\{d_w-(a-d')\}]}{A_f+[d_w-(a-d')]t_w} \tag{2.17}$$

$$\mathrm{M}_p = C_c[D - y_{sb} - 0.5a] + C^T[d - y_{sb} - 0.5(a-d')] \tag{2.18}$$

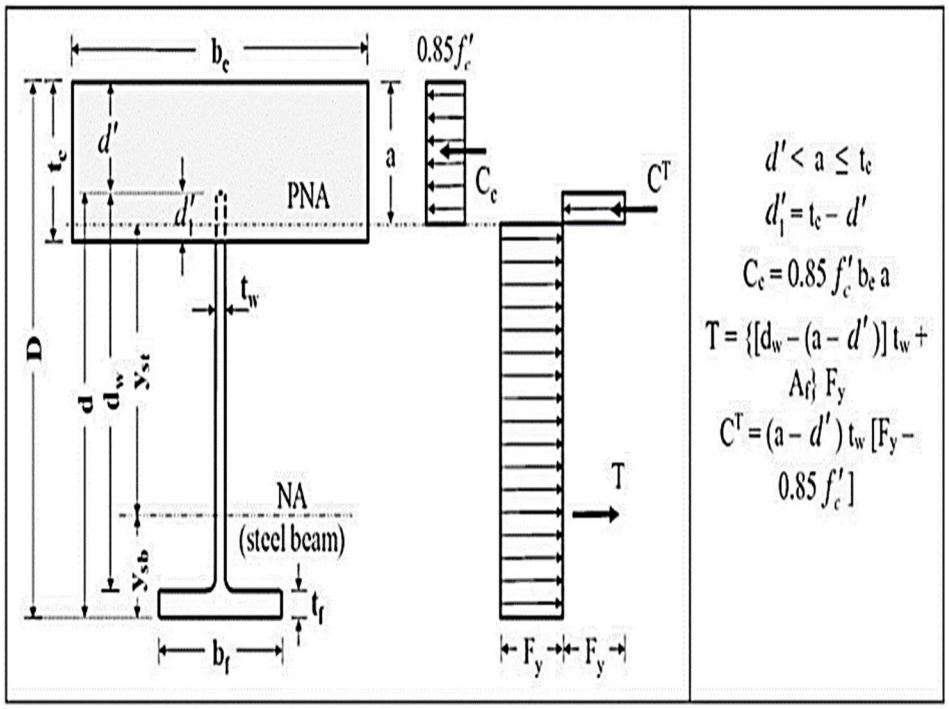

Fig. 6**.** Plastic neutral axis (PNA) is in the concrete flange, where: $d' < a \leq t_c$

Case 3:

PNA is in the web outside slab in *Fig*. 7, where: $a > t_c$

$$a^T = \frac{0.85 f'_c [d'_1 t_w - b_e t_c] + [d_w t_w - 2d'_1 t_w + A_f] F_y}{2\, t_w\, F_y} \tag{2.19}$$

$$y_{sb} = \frac{A_f[0.5t_f] + [d_w - d'_1 - a^T](t_w)[t_f + 0.5(d_w - d'_1 - a^T)]}{A_f + [d_w - d'_1 - a^T] t_w} \tag{2.20}$$

$$M_p = C_C[D - y_{sb} - 0.5t_c] + C^{T1}[D - y_{sb} - t_C - 0.5d'_1)] + C^{T2}[d - y_{sb} - d'_1 - 0.5a^T] \tag{2.21}$$

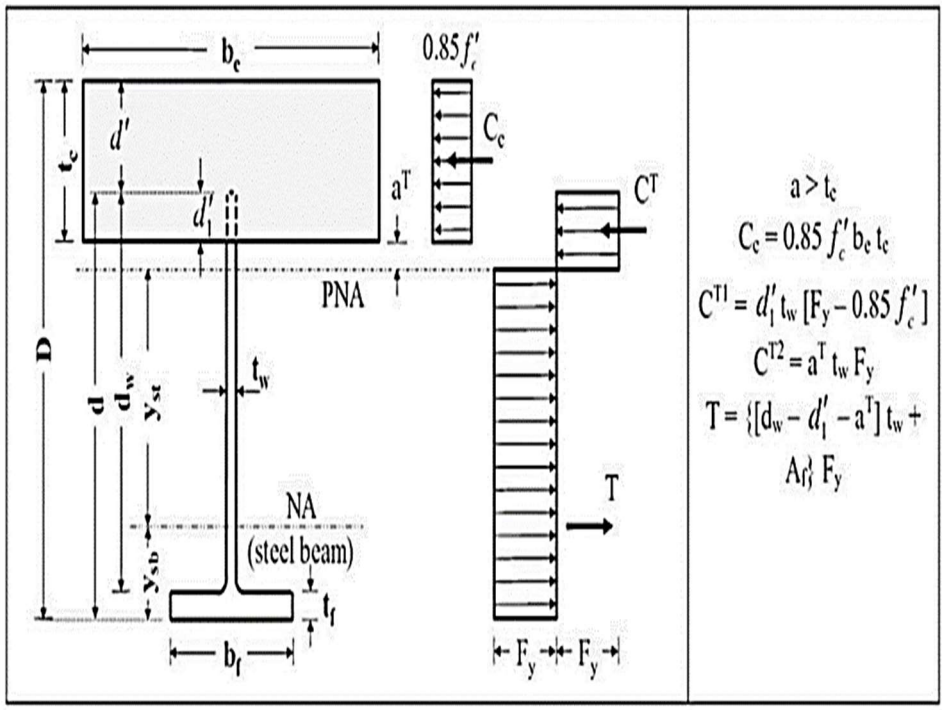

Fig. 7**.** Plastic neutral axis (PNA) is not in the concrete flange, where: $a > t_c$

3. EXPERIMENTAL MODEL

3.1. Description of experimental models

Full description of the steel-concrete composite beam model is shown in *Fig.* 8. *a, b, c* and *d.* The top reinforced concrete slab works as a concrete flange is 180 mm wide, 55 mm deep composed of 40 MPa concrete to form a 2.0 in long composite beam span as shown. It should be noted that the cross section involves the steel T-beam being embedded within the concrete slab.

The 8 mm thick steel plates were included at the ends to more accurately imitate the conditions a simply supported beam. The end plate was fixed to both ends of the steel beam through fillet welds. The end plate extended 5 mm below the steel beam and support will therefore be provided to the composite beam through the end plates. Bent R6 steel reinforcing U-bars were welded to the end plates and embedded within the concrete flange to provide a form of shear connection, connecting the end plates to the concrete flange. When subjected to bending the end plates are also expected to prevent slippage at the steel-concrete interface as the horizontal displacement of the concrete flange is to be resisted. As

seen in *Fig. 8.a* placing the applied loads closer to the center of the beam will increase the maximum bending moment.

Load was applied to the composite beams in both two-point static loading arrangements through a load cell at a rate of 0.5 mm/minute.

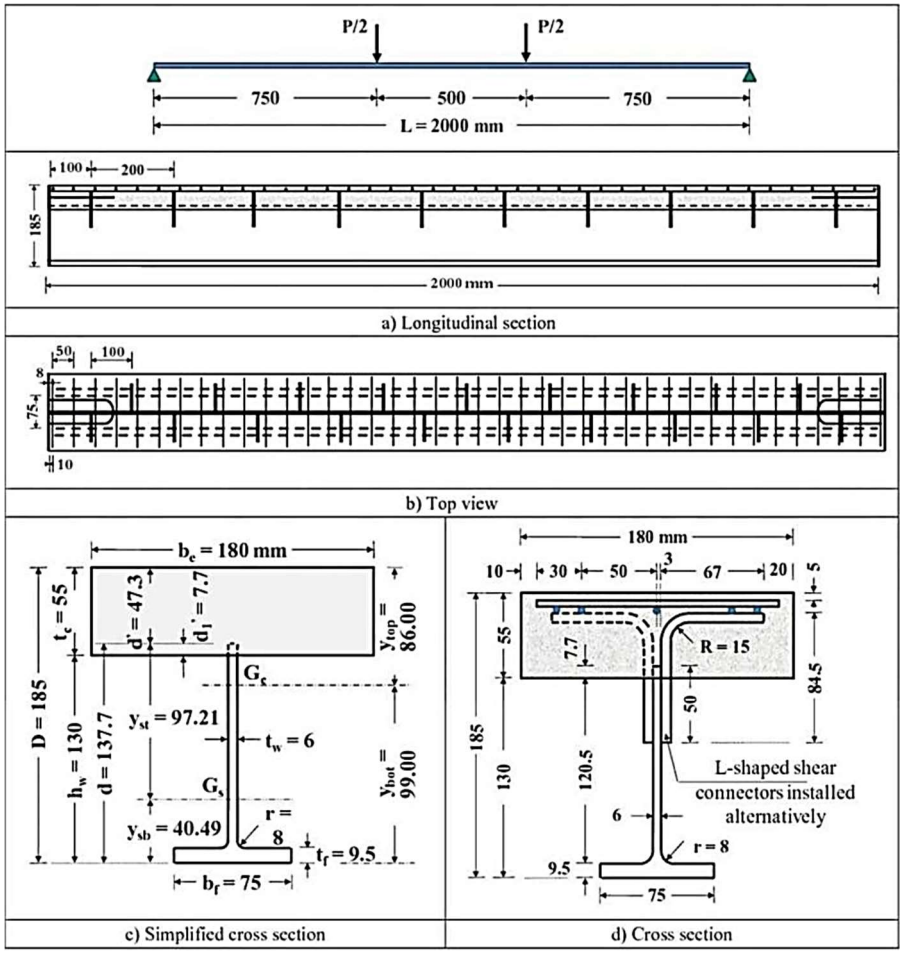

Fig. 8**.** Description of the steel-concrete composite beam model

3.2. Elastic properties of model

Equations 2.4, 2.5, 2.6 and 2.7 give neutral axis location in *Fig*. 2, moment of inertia and elastic resisting moment of the composite model:

$y = y_{top} = 8.60\ cm$, $I_{tr} = 1332.13\ cm^4$

p$M = 17.76$KN.m versus $\mathrm{M_{exp.e}} = 18.5$KN.m. therefore: $P = 47.36$KN

3.3. Elastoplastic properties of model

Equations 2.8 and 2.9 give balanced neutral axis location in *Fig*. *3,* and bending moment of the composite model and curvature in this case:

$$\frac{y_b}{0.0034} = \frac{D}{0.0034 + (F_y/E_s)}, y_b = 0.74070\,D = 13.70\ \ cm$$

$y = y_{top} = 8.60 \ll\ y_b = 0.7407(18.5) = 13.70cm$, thus, steel yields first.

The bending moment and curvature angle are :

$$M_y = \frac{210(1332.13)(10)^{-8}}{(18.5 - 8.6\rangle(10)^{-2}} = 28.26\text{KN. m.}$$

$$\Phi_y = \tan^{-1}(\frac{\varepsilon_y}{y_{bot}}) = \tan^{-1}(\frac{0.003}{18.5 - 8.60}) = \tan^{-1}(0.000303)$$

3.4. Deflection of model

Designing curve in *Fig*. *9* is derived for this model according to following steps:

$$\Delta = P[\frac{a}{24EI}\{3L^2 - 4a^2\}]\ , \frac{L}{360} = P[\frac{a}{24EI}\{3L^2 - 4a^2\}]$$

$$M = \frac{\sigma_s' I}{y_{bot}}\ , P = \frac{\sigma_s' I}{a\, y_{bot}},\ a = 75\text{ cm} \qquad (3.1)$$

$$\frac{L}{360} = \frac{\sigma_s' I_{tr}}{a y_{bot}}[\frac{a}{24EI_{tr}}\{3L^2 - 4a^2\}] = \frac{\sigma_s'}{E_s}[\frac{1}{24\, y_{bot}}\{3L^2 - 4a^2\}]$$

$y_{bot} = D - y_{top} = 18.5 - 8.60 = 9.90cm \approx 0.535D$

$$\frac{L}{D} = 0.02212\ \frac{E_s}{F_y}$$

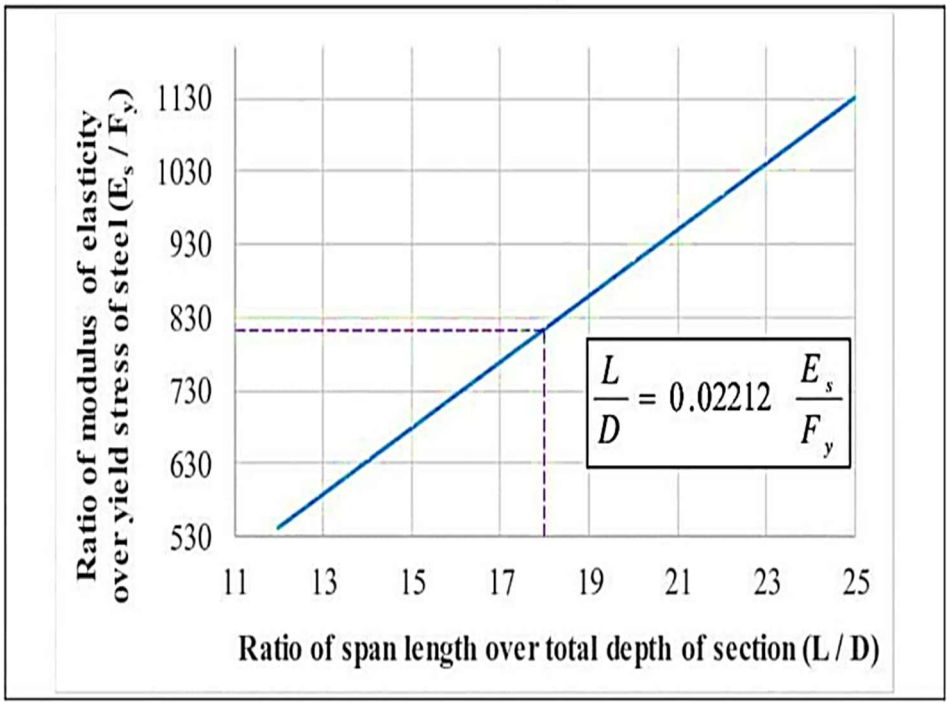

Fig. 9. Designing curve

As a guide only, the AISC (2010) Commentary suggests the following limitations:

Floor beams and girders, fully stressed, not subject to shock or vibration:

$$\frac{L}{D} = 0.0275 \frac{E_S}{F_y} \tag{3.2}$$

Floors and girders, subject to shock or vibratory loads, supporting large open areas free of partitions or other sources of damping:

$$\frac{L}{D} = 0.0250 \frac{E_S}{F_y} \tag{3.3}$$

3.5. Plastic properties of model

The plastic neutral axis, sectional forces, and plastic moment capacity according to case 2, where $d' \leq a \leq t_C$ using equations 2.16, 2.17 and 2.18 are as follow:

$a = 4.81254cm$, $y_{sb} = 4.01677cm$,$C_c = 294.527\text{KN}$, $C^T = 8.2209524\text{KN}$

$\text{MP} = 36.3684\text{KN.m}$. Versus $M_{exp.p} = 37.020\ KN.m.$

Fig. 10 shows the experiment versus theoretical calculated consequences.

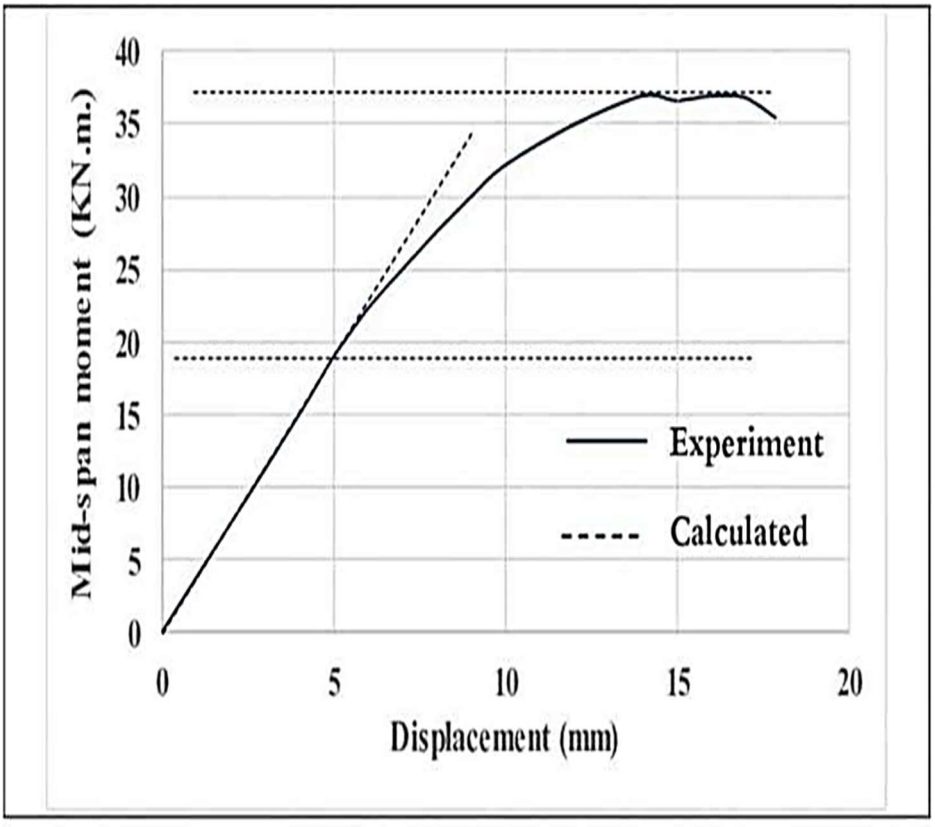

Fig. 10. Moment-deflection curve

4. CONCLUSION

Theoretical study has been done on a new-fangled steel-concrete composite beam structure with an innovative L-shaped steel shear connection. The suggested designing equations simulate the elastic, elastoplastic and full plastic experimental moments. The plastic theoretical study in case 2 coincides with the experimental behavior of the model.

Theoretical deflection study resulted in outcomes close to the test outcomes with a supportive designing curve. This curve is valuable for both designing engineers and researchers.

This type of shear connection would help to prevent separation between the concrete flange and steel beam due to the good bonding development.

REFERENCES

1. Jurkiewiez, B and Hottier, JM 2005. Static behaviour of a steel–concrete composite beam with an innovative horizontal connection. *Journal of Constructional Steel Research*, **61**, 1286-1300.
2. Leaf, D and Laman, JA 2013. Testing and analysis of composite steel-concrete beam flexural strength. *Int J Struct Civ Eng Res*, **2(3)**, 90-103.
3. Ranzi, G, Leoni, G, and Zandonini, R 2013. State of the art on the time-dependent behaviour of composite steel–concrete structures. *Journal of constructional steel Research,* **80**, 252-263.
4. Wu, J, Frangopol, DM and Soliman, M 2015. Simulating the construction process of steel-concrete composite bridges. *Steel and Composite Structures*, **18(5)**, 1239-1258.
5. Al-Shuwaili, M, Palmeri, A and Lombardo, M 2017. Efficient re-design of continuous concrete-steel composite beams. In 13 TH *International Postgraduate Research Conference* (p. 196).
6. Yang, Y, Chen, X, Xue, Y, Yu, Y and Zhang, C 2021. Shear behavior of concrete-encased square concrete-filled steel tube members: Experiments and strength prediction. *Steel and Composite Structures*, **38(4)**, 431-445.
7. Kim, DY, Ju, YG, Chun, S C, Kim, S D, Chung, KR, Lee, CH and Moon, I S 2004. *U.S. Patent No. 6,807,789*. Washington, DC: U.S. Patent and Trademark Office.
8. Amadio, C, Fragiacomo, M and Macorini, L 2012. Evaluation of the deflection of steel-concrete composite beams at serviceability limit state. *Journal of Constructional Steel research*, **73**, 95-104.
9. Ferrante, CDO, de Andrade, SAL, de Lima, LRO and Vellasco, PDS. 2020. Analytical study and experimental tests on innovative steel-concrete composite floorings. *Journal of Constructional Steel Research*, **168**, 105868.

10. He, SQ, Li, PF and Shang, F 2011. Three-dimensional simulation of steel-concrete composite beams with an interface-slip model. *In Advanced Materials Research* , Trans Tech Publications Ltd, vol. **163**, pp. 1520-1524.
11. Deretic-Stojanovic, B and Kostic, SM 2017. A simplified matrix stiffness method for analysis of composite and prestressed beams. *Steel and Composite Structures,* **24(1)**, 53-63.
12. Nzabonimpa, JD, Hong, WK and Kim, J 2018. Strength and post-yield behavior of T-section steel encased by structural concrete. *The Structural Design of Tall and Special Buildings*, **27(5)**, e1447.
13. Rana, MM, Lee, CK, Al-Deen, S and Zhang, YX 2018. Flexural behaviour of steel composite beams encased by engineered cementitious composites. *Journal of Constructional Steel Research*, **143**, 279-290.
14. Remennikov, A and Roche, M (2014). New composite construction of hybrid beams combining steel inverted T-section and RC flange. Auckland, New Zealand, *Australasian Structural Engineering Conference* (ASEC 2014).
15. Yang, Y, Xue, Y and Yu, Y 2019. Theoretical and experimental study on shear strength of precast steel reinforced concrete beam. *Steel and Composite Structures*, **32(4)**, 443-454.
16. Saari, WK, Hajjar, JF, Schultz, AE and Shield, CK 2004. Behavior of shear studs in steel frames with reinforced concrete infill walls. *Journal of Constructional Steel Research*, **60(10)**, 1453-1480.
17. American Institute of Steel Construction, Steel Construction Manual 2010. The 14th ed., *American Institute of Steel Construction*, Chicago, Illinois, 2010.
18. Johnson, RP and Anderson, D 2004. Designers' guide to EN 1994-1-1: eurocode 4: design of composite steel and concrete structures. General rules and rules for buildings. Thomas Telford.
19. British standard BS EN 10080 2005. Steel for the reinforcement of concrete – Weldable reinforcing steel.

Editor received the manuscript: 17.03.2022